Supplementary Information

Come together: on-chip bioelectric wound closure

Tom J. Zajdel[a], Gawoon Shim[a] and Daniel J. Cohen*[a]

[a] *Mechanical & Aerospace Engineering, Princeton University, 08544 Princeton, New Jersey, United States*

*Corresponding Author:
Daniel J. Cohen
Email: danielcohen@princeton.edu
Department of Mechanical & Aerospace Engineering
Princeton University
Princeton, NJ 08544

Electrochemical stability. The results of electrochemical characterization of bare silver, bleached silver, and electroplated silver electrodes are shown in Figure S1. In the case of bare silver, there is very little current until a reduction current caused by electrolytic evolution of H2 from -1.5 V to -2.0 V, accompanied by visible formation of bubbles on the working electrode. Chloridized silver electrodes ideally would sink cathodic current by the breakdown of AgCl, thus avoiding this hydrolysis reaction. The bleached silver electrode had an expected linear CV for the first cycle, but after five cycles and just 0.7 mAh of charge transfer, the CV reverted to that of bare silver, as the chloridization layer has been consumed. The electroplated electrode shows a robust response that is nearly unchanged throughout 2.1 mAh of charge transfer throughout these five cycles. Because current delivered in the convergent field device under normal operation ranges from 6-8 mA, the equivalent current sunk by a cathode must be at 72-96 mAh for a 12 h experiment. That means that bleached silver electrodes are not sufficient for high, sustained current deliveries, and electroplated silver electrodes should be used instead, since a much larger AgCl volume can be plated onto the cathode than is formed by bleach immersion.

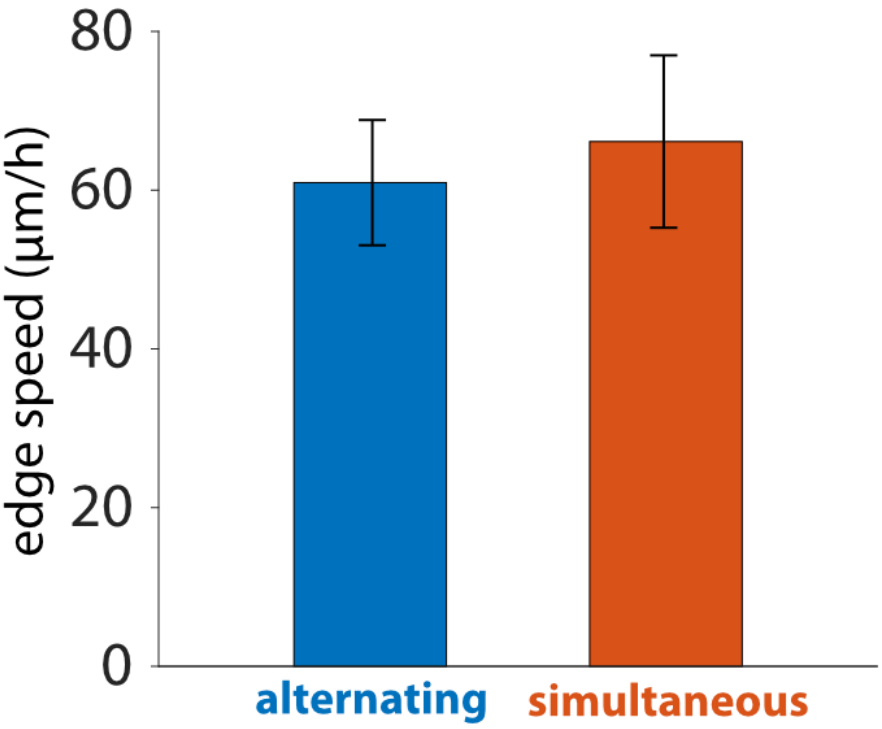

Figure S1. Edge expansion speed compared between alternating stimulation side every 30 seconds and simultaneous stimulation. Edge expansion speeds averaged over an 8 h period. The average edge expansion was 61.0 ± 7.9 µm/h and 66.1 ± 10.9 µm/h for the alternating and simultaneous cases, respectively. N = 6 and N = 2 edges, respectively. Error bars represent standard deviation.

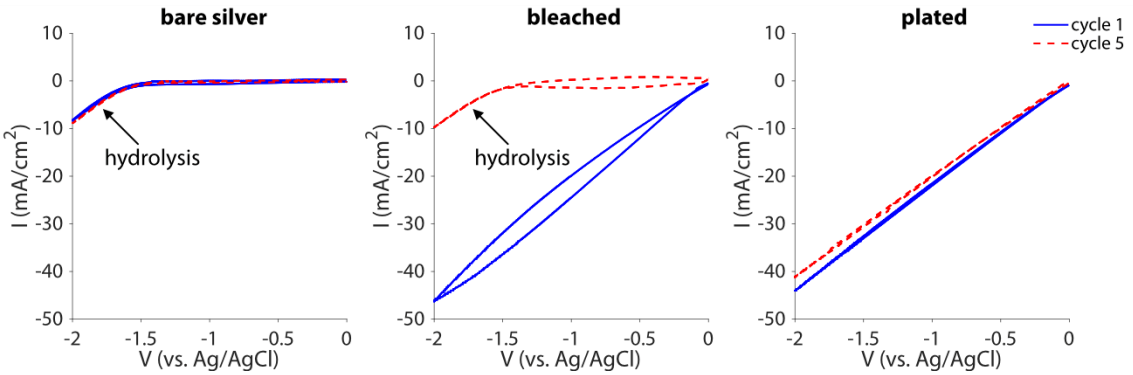

Figure S2. Electrochemical stability of three different cathode preparations, each probed by cyclic voltammetry. Cyclic voltammograms measured by a potentiostat in a three-electrode system. The working electrode was made from the material under test, cut to an area of 3 cm^2. The counter electrode was a large silver chloride foil (15 cm^2 area), and the reference was a standard Ag/AgCl electrode. Five consecutive voltage sweeps were performed at a 100 mV/s scan rate from 0 to -2 V vs. Ag/AgCl. The first (solid blue line) and fifth (dashed red line) cycles are presented. The operating point of the cathode during standard device operation is -1.5 to -1.7 V vs. Ag/AgCl. At this voltage, bare silver produces faradaic current via hydrolytic evolution of hydrogen gas. Chloridizing the silver enables the electrode to source high faradaic current via the cathodic breakdown of AgCl at these voltages, avoiding potentially harmful pH shifts caused by hydrolysis. However, the method of chloridization matters, as bleach-immersed AgCl electrodes were stripped by the fifth cycle while electroplated AgCl electrodes lasted longer.

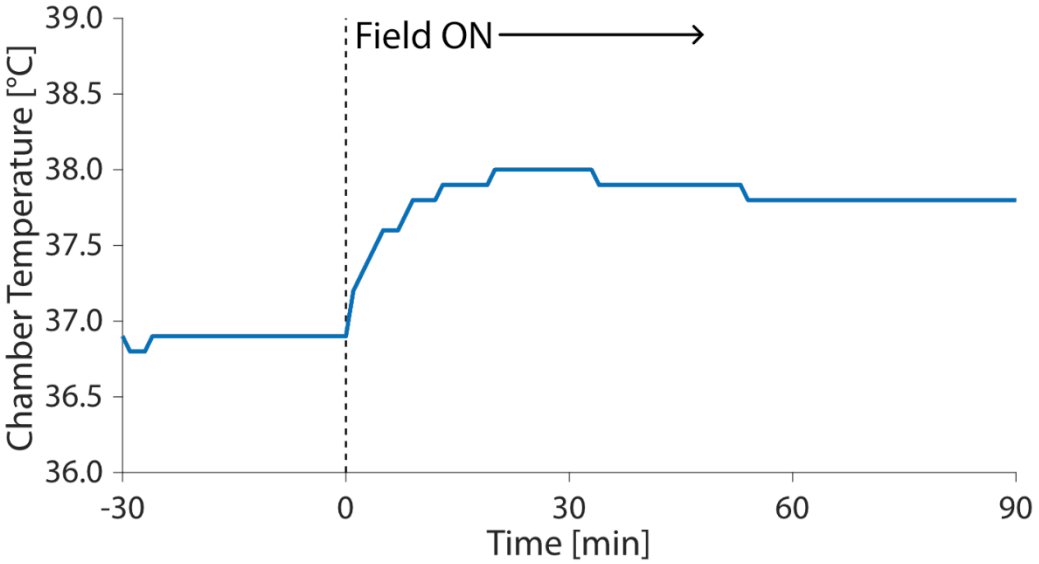

Figure S3. Temperature stability of device during stimulation. Temperature measured by inserting a thermocouple into device's outlet port during perfusion. Stimulation field turned on at t = 0, marked by the dotted line. After the onset of stimulation, the system temperature reaches steady state in ~15 min, resulting in a temperature increase of ~1 °C due to Joule heating.

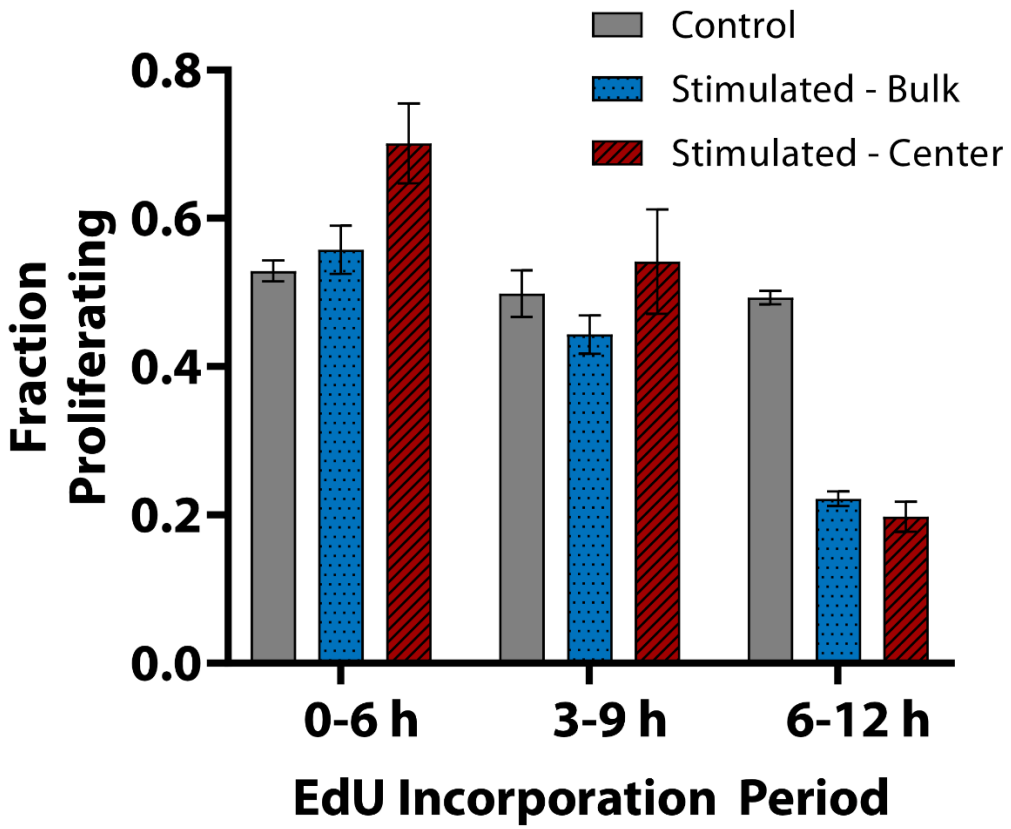

Figure S4. Time course of cell proliferation as assayed by EdU incorporation. Fraction proliferating is the ratio of the number of cells that incorporated EdU over the total population. After the onset of stimulation, cell proliferation rate decreased slowly and persistently as compared to the non-stimulated control. Bulk control tissue results averaged across N = 8, 8, and 4 samples for EdU incorporation periods of 0-6 h, 3-9 h, 6-12 h respectively. Bulk stimulated tissue results averaged across N = 4 samples for each time point. Central stimulated tissue results averaged across N = 2 samples for each time point. Error bars represent standard deviation.

Video Files and Captions

All videos are separate files and can be found at the following link: **https://www.dropbox.com/sh/4c7645jvv9aiqv1/AAArNoES4GmO0NK-hcPp6sfPa?dl=0**

Video 1. Time-lapse movie showing migration of convergently stimulated tissues versus control tissues. In the electric stim case (right), a convergent field was applied towards the center gap for 12 hours, alternating stimulation between the left and right tissues every 30 seconds. In the control case (left), tissues were imaged in the device for 12 hours without stimulation. Keratinocyte cells were stained by a lipophilic Cy5 dye (imaged with $\lambda_{ex}/\lambda_{em}$ 644/665 nm).

Video 2. Time-lapse movie of converging keratinocyte monolayers. Following a 30-minute control period, a convergent field was applied to the center for 12 hours, alternating stimulation between the left and right tissues every 30 seconds. Cells were stained by a lipophilic Cy5 dye (imaged with $\lambda_{ex}/\lambda_{em}$ 644/665 nm).

Video 3. Time-lapse movie of convergence zone of a convergently stimulated keratinocyte monolayer. A convergent field was applied to the center of a confluent monolayer for 6 hours, alternating stimulation between the left and right half every 30 seconds. Cells were stained by a live nuclear dye (imaged with $\lambda_{ex}/\lambda_{em}$ 358/461 nm).